J. exp. Biol. (1982), 101, 307–319
With 5 figures
Printed in Great Britain

THE MORPHOLOGY AND PASSIVE ELECTRICAL PROPERTIES OF CLAW CLOSER NEURONES IN SNAPPING SHRIMP

BY JOHN A. WILSON AND DEFOREST MELLON, JR
Department of Biology, Gilmer Hall, University of Virginia, Charlottesville, VA 22901

(*Received* 1 *June* 1982 – *Accepted* 4 *July* 1982)

SUMMARY

1. The morphology and passive electrical properties of the dimorphic pincer and snapper claw closer neurones were examined in the snapping shrimp, *Alpheus heterochelis*.

2. No differences were found between homologous pincer and snapper neurones for input resistance and length constant in the proximal portion of the axons, or for the proximal axonal and dendritic anatomies using intracellular cobalt staining.

3. To determine the effect of cell body size upon the passive electrical properties of the neurones, we modelled the neurones by computer. The difference in cell body size causes less than a 3% change in the electrical properties of the neurone at the axon root.

4. Thus, despite the striking behavioural dissimilarities between the pincer and snapper claws, there is no electrical or morphological basis in the claw closer neurones for this difference.

INTRODUCTION

Morphological restructuring within adult arthropod nervous systems is, in general, limited to an increase in the size of existing neurones and the addition of sensory neurones. The ability of adult Alpheid shrimp to transform a pincer claw into a behaviourally and morphologically different snapper claw following the loss of the original snapper is thus of interest. The transformation is particularly dramatic because the pincer, which closely resembles the claws of lobsters and crayfish, enlarges to more than four times its original size and takes on a different shape which includes a plunger and socket used in snappings. This dimorphism could be associated with major functional changes within an adult central nervous system during claw transformation. The phenomenon of claw transformation was originally described by Przibram (1901) and Wilson (1903) and has been recently reviewed by Mellon (1981). Wilson (1903) and Mellon & Stephens (1978) have clearly demonstrated that simply transecting the nerve trunks to the claw can cause or prevent claw transformation. These findings not only implicate the nervous system in initiating claw transforma-

tion, but also raise the question of whether neuronal modifications accompany the other physiological and anatomical changes that occur during claw transformation.

Transformation of a pincer claw into a snapper claw has been shown to include physiological modifications of the muscle and neurones. During claw transformation, the terminals of closer motor neurones undergo physiological modifications, including a change from poorly facilitating to moderately facilitating release of transmitter (Stephens & Mellon, 1979). Moreover, there are obvious, but not absolute, behavioural differences in usage of the two claws (see Ritzmann, 1974). Since Govind & Lang (1981) have recently shown that the claw motor neurones of the lobster show an asymmetry in response to sensory stimulation which may contribute to the different behavioural uses of the lobster claw, claw transformation may also result in changes in the physiological properties of the claw closer motor neurones. Finally, dramatic reversible differences occur in the sizes of the cell bodies of homologous motor neurones supplying the closer muscles of pincer and snapper claws (Mellon, Wilson & Phillips, 1981).

We have characterized the closer motor neurones of the snapper and pincer claws on the basis of their proximal input resistances, electrical excitability and axonal and dendritic morphology. We find them to be similar, despite the differences in cell body size: an effect predicted by computer modelling. We interpret these findings as demonstrating that the claw motor neurones need only undergo minor functional changes for claw transformation to occur.

METHODS

Alpheus heterochelis were obtained from Gulf Specimen Co., Panacea, Florida at monthly intervals and were maintained in artificial sea water at 22–26 °C. Relatively large individuals were used (> 4 cm in length) with large, highly dimorphic claws, indicating that they had not undergone recent transformation. The animals were cooled to 4 °C for ½–1 h prior to dissection.

The tendon of the basi-ischiopodite levator muscle in the cheliped was then cut to prevent autotomy (McVean, 1974). The animal was secured, on its side, in a dissecting dish and covered with cold, oxygenated, artificial sea water. The carapace overlying the first three gills was removed together with the gills and the gill bailer. The coxal muscles of the cheliped were exposed and then cut away until the ganglion and the two nerve roots were exposed. (This lateral approach precluded studying neurones from both sides of a single animal, but allowed us to maintain the animal for several hours.) Extreme care was taken not to damage the haemolymph supply to the ganglion, as this invariably caused death within 10 m. The cheliped was secured to the dish and two holes were made in the propus, one for stimulating electrodes and the other for an intracellular recording electrode. The ganglion and the nerves were then illuminated using a small fibre optic light guide oriented parallel to the nerve trunks. This illumination sometimes highlighted the larger axons.

Stimulating and recording techniques. Claw motor neurones were stimulated extracellularly using a pair of 50 μm copper wires insulated except at their tips. These electrodes were inserted into the proximal portion of the propus, because from this

location the unmyelinated terminals of the axons could be reliably stimulated. This method was unsuitable for stimulation of axons in the nerve trunks due to their heavy myelin wrapping (Ritzmann, 1974 and Kusano, 1967). Intracellular recordings from the claw closer muscles were made using glass microelectrodes filled with 3 M-KCl and having resistances in the range 10–25 MΩ. Double-barrel microelectrodes were made by positioning two fibre-filled capillary tubes close to one another with heat-shrink tubing, heating and rotating the joined tubes through an angle of 185–195°, and then pulling the fused pair. The resistances ranged from 10 to 35 MΩ when electrodes were filled with 3 M-KCl. Coupling between barrels was minimal: 20 nA of current passed into one barrel caused less than 1 mV displacement in the other one in earthed sea water.

Intracellular recordings from muscle fibres were verified by noting a sudden negative shift in the electrical potential and the appearance of junction potentials in response to stimulation of the motor axon. Penetrations of closer motor axons with double-barrel microelectrodes were made 50–500 μm from where the peripheral nerve root left the ganglion. Impalement of a neurone was indicated by the presence of a resting potential of −50 to −80 mV, relative to earth. Spikes of 70–100 mV were recorded in response to both antidromic and orthodromic stimulation. The neurone was then assigned a preliminary identification by its effect upon the muscle fibre. A series of current pulses (500 ms duration) was passed into the axon and the resultant voltage change was measured to obtain an I–V relationship. To determine the length constant, a second, single-barrel electrode was used to impale the neurone at a measured distance distally from the primary recording site. Current was passed from one barrel of the double-barrel microelectrode, and was recorded with the other barrel and the independent electrode, providing us with the voltage decrement over a known distance of what we assumed to be semi-infinite cable.

Intracellular staining. Intracellular staining was achieved by filling one barrel of a double-barrel micropipette with either 150 mM $CoCl_2$ in 2·7 M-KCl, 4% Lucifer Yellow, or (optimally for these neurones) 500 mM-$Co(NO_3)_2$. After physiological identification and examination 10 Hz current pulses of 50 ms duration (ranging from 10 to 100 nA for cobalt-filled electrodes) were applied through this electrode for 1–2 h. The suboesophageal and thoracic ganglia were then removed from the animal and the cobalt was precipitated using 1 ml of commercial ammonium sulphide solution in 9 ml of sea water for 10 min. The ganglia were rinsed in sea water and fixed for 1–2 h in buffered 10% formalin and then transferred to 70% alcohol for at least 12 h to remove any excess formalin. They were passed through a descending alcohol series and directly into a Timms' developer (Tyrer & Bell, 1974) which had a modified composition (4·5% gum acacia, 10% sucrose, 0·43% citric acid, and 0·17% hydroquinone). After 1 h in the developer in the dark at 50 °C, 1 ml of freshly made 1% $AgNO_3$ was added to 9 ml of developer and intensification was carried out until the ganglion was a tobacco brown colour (20–50 m). The tissue was transferred to warm developer which did not contain silver and allowed to cool to room temperature in the dark. It was then dehydrated in an alcohol series and cleared in methyl salicylate. After initial observations were made of the whole mount, the tissue was transferred to propylene oxide and embedded in a soft resin containing Embed 812, 31 ml, DDSA,

50 ml, and DMP-30, 1·2 ml. It was then serially sectioned at 50 μm using a sliding microtome, coverslipped using resin, drawn by means of a camera lucida, and photographed. Stained neurones were reconstructed with the aid of a Wild microscope and drawing tube. The alignment of sections in the emerging reconstruction was judged by eye. Measurements were made of the diameters of the primary neurites at 50 μm intervals from the cell body to the last branch point of the neurone within the ganglion, and the measurements were averaged. The length and number of large (diameter greater than 3 μm) branches leaving the primary neurites were determined. Axonal diameters were measured every 200 μm beyond the exit of the nerve root from the ganglion for at least 800 μm.

Model. The computerized model was supplied and modified for these neurones by Dr William H. Calvin. A detailed description of the model is provided in Turner & Calvin (1981). The model is based upon the analysis of neuronal cable properties by Rall (1959). From our quantified anatomical data the processes of the neurones were treated as finite lengths of core-conducting cable of specified lengths and diameters. The neurone was considered to be at steady state; thus capacitative and voltage transients could be excluded, and the extracellular voltage gradients approach zero, since we assume they should be equal for both sides of the ganglion. Since the morphology of the segments were from our data, the 3/2 rule of Rall (1962) and Rall & Rinzel (1973) was not assumed. Calculations were carried out using a generally recognized median value of 90 ohm-cm for R_i, and the value of R_m was varied from 800 to 50,000 ohm cm^2; the cell body diameters were taken as 60 and 75 μm for the pincer and snapper closer exciters, respectively (Mellon *et al.* 1981). The input resistance of the axon was calculated and the effect of conductance changes at specific sites along the neurone was computed, using the equations of Rall (1959). The values obtained from the computer reconstruction were then compared with our physiologically measured results.

RESULTS

The claw closer muscles each receive axon terminals from two excitatory motor neurones (closer exciter 1 and 2) and two inhibitory neurones (lateral and dorsal inhibitors) (Mellon & Stephens, 1979; Mellon *et al.* 1981). The closer exciter 1 innervates most, if not all, of the muscle fibres in the major closer muscle (Mellon & Stephens, 1979) and closer exciter 2 innervates a small percentage of the major closer muscle fibres. Closer exciter 2 innervates all of the minor closer muscle fibres (Mellon & Stephens, 1979). The two inhibitors were found to innervate many muscle fibres of the claw closer muscles. We did not determine whether or not the two inhibitors innervated other muscles. The density of innervation of muscle fibres was greatest in the most medial closer muscle fibres. Although the dorsal and lateral inhibitors are clearly different anatomically (see below), they were also physiologically distinguishable from each other. Large frequent spontaneous depolarizing postsynaptic potentials (PSPs) were recorded in the proximal portion of the axon of the lateral inhibitor but not in the dorsal inhibitor.

Electrical properties. The electrotonic properties of the motor neurones were investigated using double-barrel electrodes. After impaling an axon, antidromic stimula-

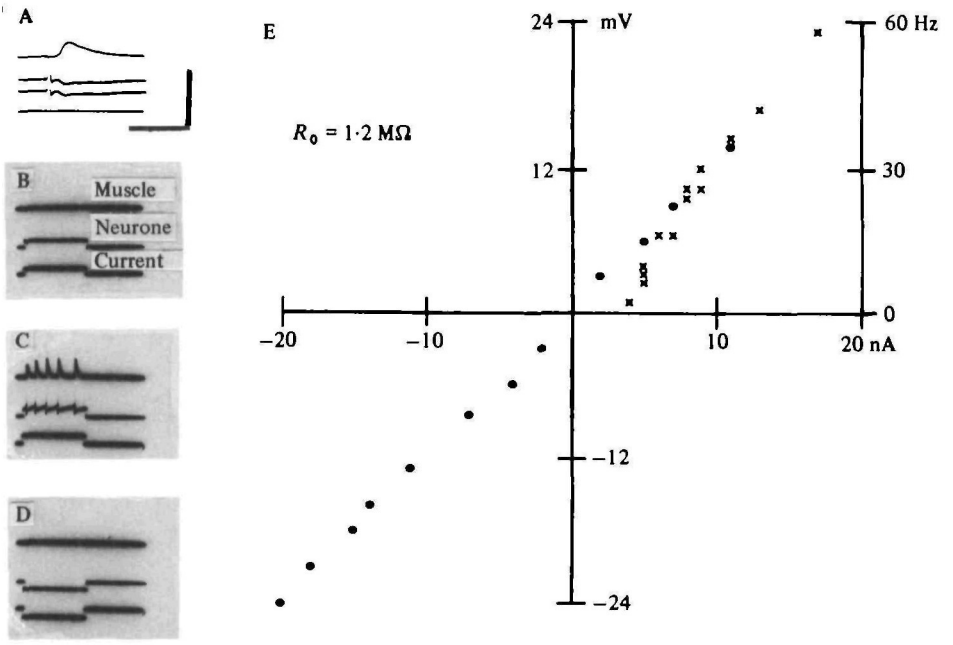

Fig. 1. Electrical records, current–voltage and current–frequency characteristics of a snapper closer exciter 1 motor neurone. (A) Peripheral stimulation of the neurone caused an EJP in the muscle (top trace) and antidromic spikes of identical amplitudes in both barrels of the recording electrode in the axon (4th trace current monitor). (B) Effect of sub-threshold depolarizing current (third trace) passed from one barrel (not shown) of the microelectrode upon the neurone. Since the impulse threshold was not reached, the muscle was not affected. (C) Suprathreshold current caused the neurone to produce 5 impulses, and the large EJPs in the main closer muscle allow identification of the neurone as closer exciter 1. (D) Inward current caused a measurable hyperpolarization of the neurone. (E) The effect of injected current upon the membrane potential (○) and spike frequency (×) is illustrated. The slope of the current–voltage plot was used to calculate the input resistance (1·2 MΩ). Calibrations: all intracellular neurone traces 50 mV, all intracellular muscle traces 20 mV, current 50 nA; time bar: *A* 50 ms, B-D 500 ms.

tion was used to ascertain that both barrels of the electrode recorded impulses and spontaneous synaptic potentials of equal magnitude as shown in Fig. 1 A.* A series of depolarizing and hyperpolarizing current pulses was then passed through one barrel and the resultant transmembrane voltage values were recorded through the other barrel. Records and the related current–voltage curve are shown in Fig. 1 B–E. The slope of the curve was used as the value of input resistance for each neurone studied. Input resistances for individual neurones ranged from 1·2 to 8 MΩ (see Table 1). The mean values for the snapper and pincer neurones are not statistically different, and the variations in input resistance are of the same magnitude as those reported by Mellon & Kaars (1974) for crustacean sensory axons of similar diameter. We also examined the threshold and current–impulse frequency relationships for

* We made certain that all of the previously stated criteria were met, as Kusano (1967) found that positive-going spikes could be recorded from the region between the myelinated sheath and the axon of Kuruma shrimp giant fibres. We did this to be certain that we were within the neurone, because in one case before we adopted these criteria, only the region of axon surrounded by one glial cell was obtained.

TABLE 1. *Neurone input resistances* (MΩ)

	Snapper	Pincer
Closer exciter 1	1·2	2·5
	4·0	5·0
	5·25	5·0
	5·0	
Mean	3·86	4·17
Closer exciter 2	6·0	6·6
	2·7	3·3
	3·0	2·0
Mean	4·25	4·63
Lateral inhibitor	8·0	8·0
	3·0	3·0
	4·0	
	3·2	
	5·0	
	3·0	
Mean	4·37	4·67
Dorsal inhibitor	5·0	5·0
	3·6	7·5
	5·0	3·0
	4·0	
Mean	4·40	5·17
Grand means	4·17 S.D. 1·54	4·63 S.D. 2·06

these neurones. In all cases the current threshold was between 2 and 7 nA and spike frequency increased approximately linearly with current up to 20 nA. Again we found no consistent difference between the snapper and pincer neurones.

We were interested in the extent to which the lumped resistive properties of the central branches of a motor neurone contributed to our measurements of (proximal axonal input resistance. If the measured length constants were short (less than 0·5 mm, given our recording site), clearly we would be forced to assume that our measurements applied only to the local axonal region. If, on the other hand, the length constants were larger than 1·0 mm (more than the distance from our most distant recording site to the cell body), a potential would exist for major contributions to the input resistance at our recording site by the central branches of the claw closer neurones. We were able to penetrate the same neurone with a single-barrel electrode and a double-barrel electrode on two occasions, and the estimated length constants of these neurones were 1·2 and 2·2 mm. These values are larger than the measured distance from our most distal recording site to the extremes of the central arborization (see anatomy below); thus our recording site may have been electrically close to the dendritic arborization. Since the central arborization of the neurones may affect the parameters close to the ganglion, we measured the input resistances of more distal regions of the axon. In the two cases in which we were able to penetrate the same neurone and record equal resting potentials and spike heights at both sites, the input resistance was the same at both recording sites (3·0 and 5·0 MΩ for these two neurones). These findings suggest that the input resistance of the neighbouring dendritic branches matches that of the axon.

Anatomy. We next sought to determine whether or not functional similarities in the

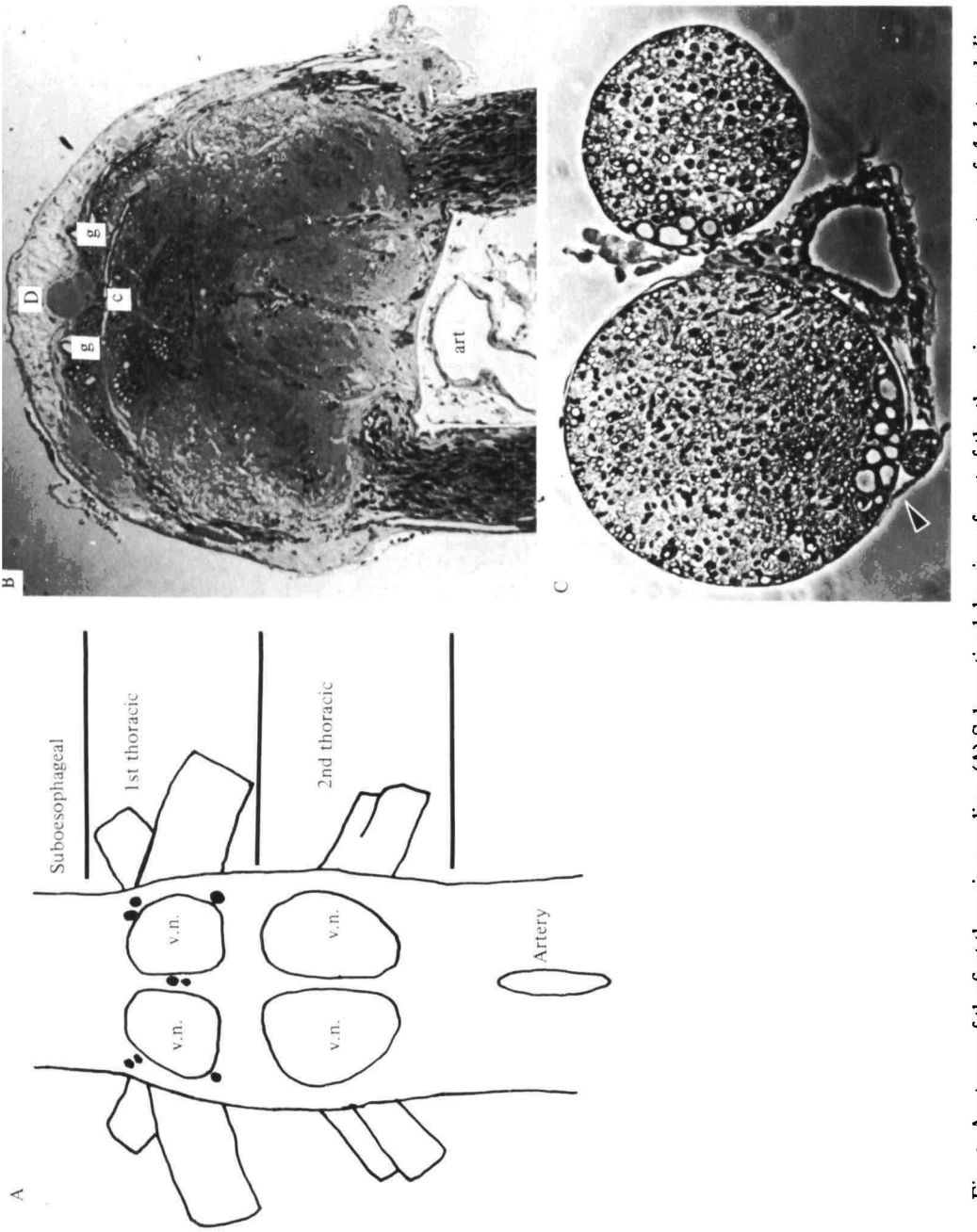

Fig. 2. Anatomy of the first thoracic ganglion. (A) Schematized drawing of part of the thoracic nervous system of *A. heterochelis*. The location of the cell bodies of the eight claw closer motor neurones and their relationships to the ventral neuropils (v.n.) are shown in the first thoracic ganglion. (B) Low-power micrograph of a 2·5 μm cross-section of tissue fixed in buffered glutaraldehyde through the ganglion at the level of the dorsal inhibitors (D). Medial giant interneurones (g) and a commissure (c) and the ventral artery (art) are also shown. (C) Cross-section of the snapper claw nerve trunks approximately 200 μm after leaving the ganglion. The bundle containing the four axons to the closer muscle is indicated with an arrow.

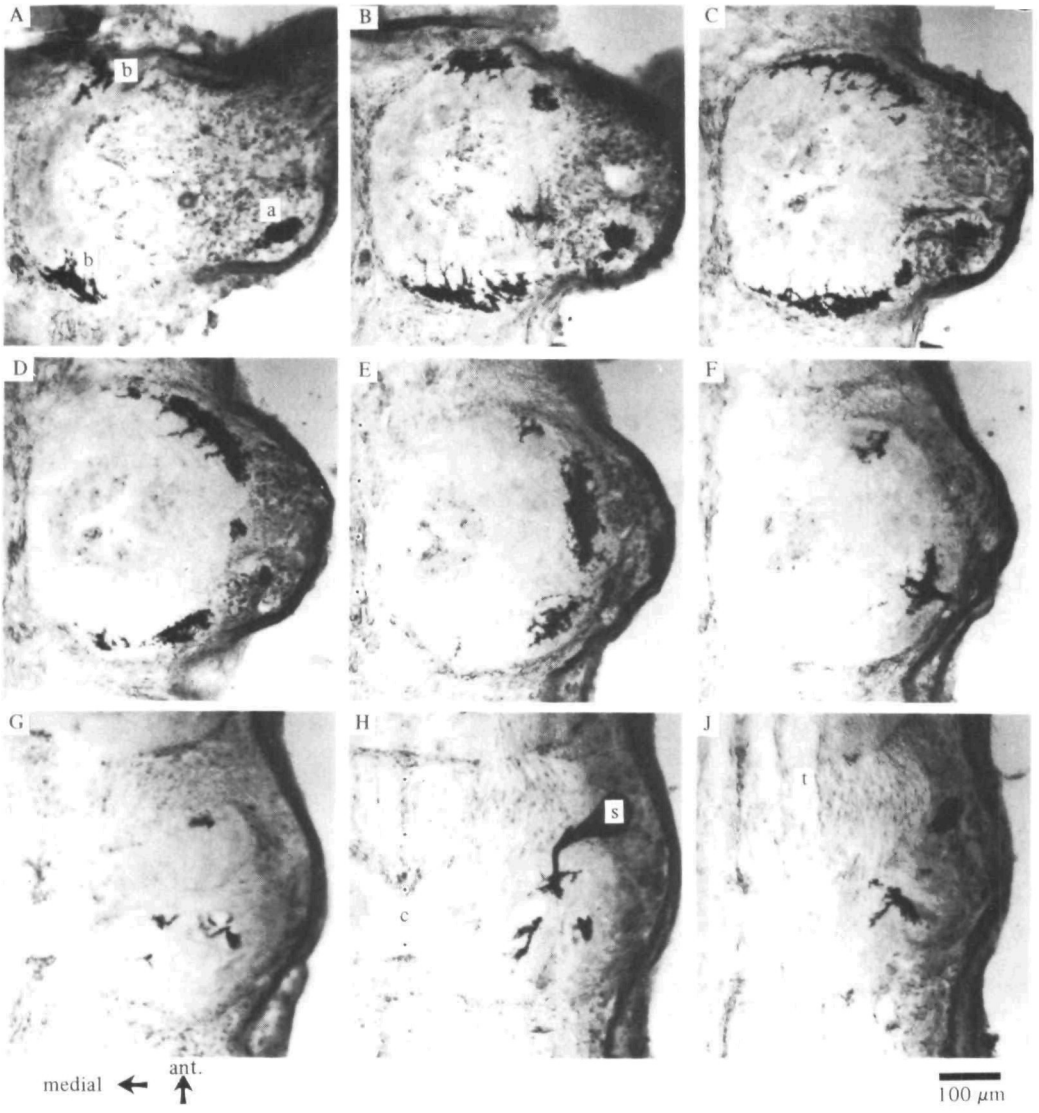

Fig. 3. Nine of 16 50 μm serial coronal (ventral–dorsal) sections through a ganglion in which the motor neurone (snapper-closer exciter 1) was stained with cobaltous ions. (A–E) The biramous major branches (b) of the neurone are found near the midline in A (the 2nd most ventral section), and in successively more dorsal sections the branches are seen more laterally. The axon (a) begins to decrease in diameter in sections C and D. (F) The axon, the biramous major branches, and the process to the cell body are all seen to have joined. (G) The ventral-most commissure (c) and through tracts (t) are seen, and in sections H and J are the cell body (s) and the termination of the ventral neuropil. Dots in E and H indicate midline.

laterally homologous motor neorones were matched by identical anatomical details. Intracellular injection of cobalt ions was used to examine this question. The motor neurones of the claw closer muscles are contained within the first thoracic ganglion. This ganglion is fused with the suboesophageal one and, posteriorly, with the second thoracic ganglion, (Fig. 2A). Because the thoracic ganglia are fused, there are several anatomical differences in the organization of the shrimp first thoracic ganglion as compared with those of the crayfish (Wiens, 1976) and spiny lobster (Silvey, 1981). We will therefore briefly illustrate the major differences.

The ganglion lies atop a large blood sinus and artery (Fig. 2B) with which it is connected by many smaller vessels. The ganglion is readily divided into a dorsal and a ventral portion on the basis of distinguishable anatomical features. The dorsal portion is characterized by several interganglionic tracts which travel through it and are comprised of groups of myelinated fibres (Fig. 2B). The paired medial giant axons are easily distinguished along the dorsal surface of the ganglion (Fig. 2B). The lateral giants are not always readily distinguishable. The dorsal portion of the ganglion also contains all the commisures which connect the two sides of the ganglion (Fig. 2B). The ventral portions of the ganglion are two ovoid regions of neuropil surrounded by blood sinuses and connective tissue. The ventral neuropil is composed predominantly of unmyelinated processes. Large-diameter processes occur only near the edge of the ventral neuropil, whereas in the centre only very small (0·1–2·0 μm) processes are seen. Neurone cell bodies are found primarily in the anterior and posterior regions of the ganglion, although two large cell bodies are found along the dorsal midline (Fig. 2B).

There are no apparent differences between the two sides of the ganglion. The primary difference between the organization of the crayfish 1st thoracic ganglion (Wiens, 1976), the spiny lobster 3rd thoracic ganglion (Silvey, 1981), and the snapping shrimp 1st thoracic ganglion, is that the lateral regions of the crayfish and spiny lobster ganglia correspond to the ventral neuropil of the shrimp. This means that the shrimp motor neurones appear to have been rotated ventrally and medially. Two nerve roots leave the ganglion from each side along its lateral ventral margin. It is in this region that the axons become myelinated and assume the appearance seen in more distal portions of the root (Fig. 2C). The nerve roots each have a group of larger myelinated fibres (Fig. 2C) and the rest of the root is comprised of smaller fibres. The finding that there is a group of large fibres which are the motor neurones in the nerve trunks agrees with Silvey's (1981) finding that the larger fibres are motor neurones.

Structural relationships between the closer neurones and the ganglion were studied from serial microscope sections (Fig. 3). The entire ganglion was contained in 16 50 μm coronal sections, and the closer neurone was confined to the 10 most ventral sections. Starting with the second section from the ventral edge (Fig. 3A), the axon (defined here as the process which proceeds peripherally after all central branching has ended) is seen laterally (to the right in the figure), and the dendritic branching is found anteriorly and posteriorly near the midline of the ganglion in the cortex of the ventral neuropil. Subsequently (Fig. 3B–E), the axon travels dorsally, decreases in diameter, and loses the myelin wrapping it possessed more ventrally. In Fig. 3F the

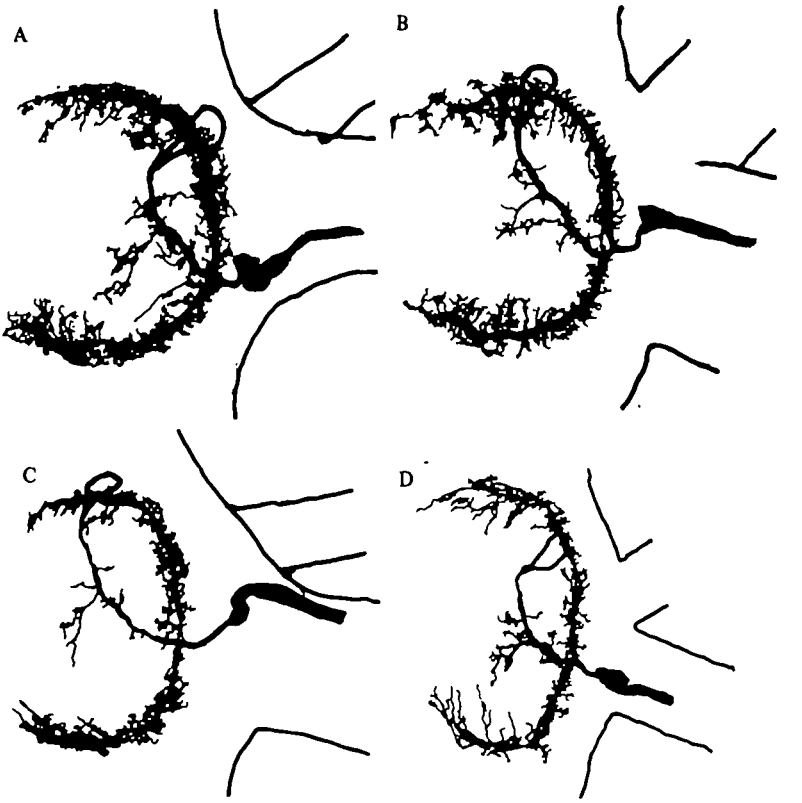

Fig. 4. Anatomical reconstructions of the four closer exciter neurones as viewed from above. (A) The snapper-closer exciter 1, shown in section in Fig. 3, is here reconstructed and presented next to B, of the pincer-closer exciter 1. (C) The snapper closer exciter 2 and (D), the pincer-closer exciter 2 are shown. The neurones have been scaled such that the anterior to posterior distance across the ventral neuropil is equal in each case, thus removing the effect of differences in the size of the whole animal.

axon and the main anterior and posterior branches fuse with the process from the cell body. It should also be noted that in sections A–F all of the branching occurs in the cortex of the ventral neuropil. The subsequent three sections show the cell body and its process (Fig. 3 G–J). In this region the ventral neuropil terminates, and the tracts and commissures of the dorsal neuropil become visible. Here, as more ventrally, all of the branching is very compact and occurs in the outermost 100 μm of the ventral neuropil. All of the finest branches terminate within 150 μm from their point of departure from the larger branches. The shrimp closer exciter motor neurones' branches are found more ventrally than those of the spiny lobster (see Silvey, 1981, fig. 1), and this appears to be related to the different location of the neuropil. Also it should be noted that the branches in the shrimp neuropil are restricted to the cortex of the neuropil.

Fig. 4A is a reconstruction of the neurone shown in Fig. 3. A similar reconstruction of the homologous motor neurone to the pincer is shown in Fig. 4B. Aside from the previously reported difference in cell body diameter (snapper exciter mean circumference 207 μm, pincer exciter mean circumference 184 μm, Mellon *et al.* 1981), we

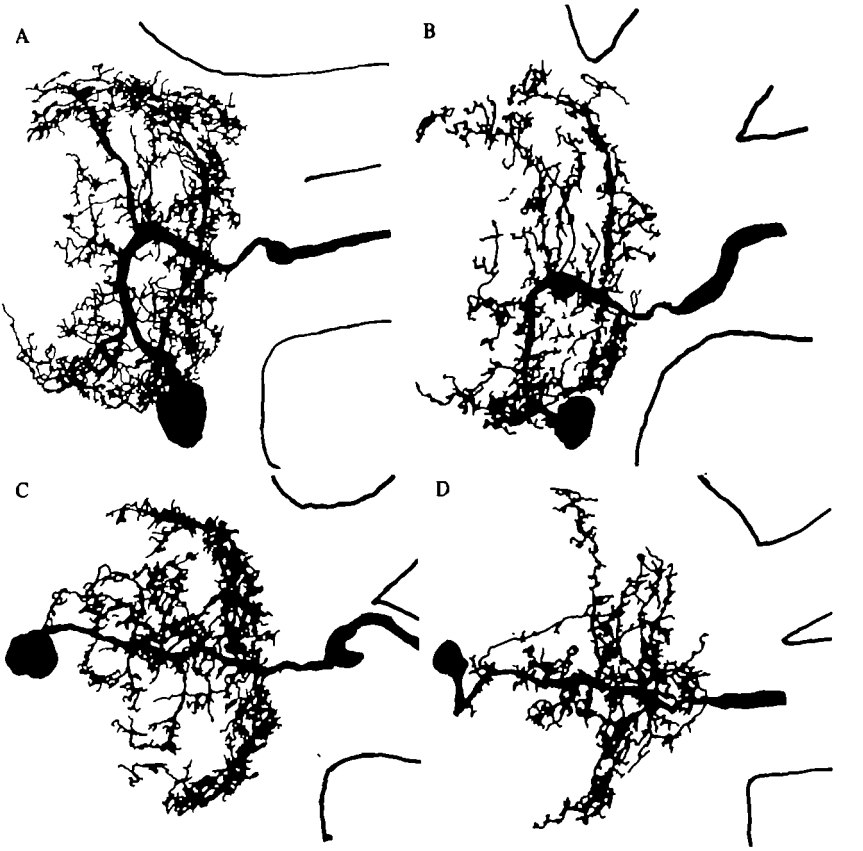

Fig. 5. Claw closer inhibitor neurones are shown in coronal views scaled as in Fig. 4. (A) Snapper and (B) pincer lateral inhibitors. (C) Snapper and (D), pincer dorsal inhibitors. Here, as with the exciters, the similarities of the contralateral homologous structures predominate; however, the larger sizes of the snapper neurone cell bodies are evident.

found no major anatomical differences between these contralaterally homologous neurones. Both neurones branch in the same regions, have primary neurites to which the cell body is attached with the same diameter (snapper 8·8 μm S.D. $\pm$ 2·5, pincer 9·0 μm S.D. $\pm$ 3·1), proximal axons with the same average diameter (snapper 18·6 μm S.D. 6·6, pincer 19·7 μm S.D. 3·8), and cell bodies in the same location. The snapper and pincer closer exciter 1 motor neurones are, in fact, so similar that drawings of these neurones can be superimposed such that there are only very small regions not in perfect register. Comparisons of the snapper (Fig. 4C) and pincer (Fig. 4D) closer exciter 2 motor neurones also fail to reveal any quantifiable difference other than the previously mentioned difference in cell body size. Thus the snapper and pincer closer exciter motor neurones have branching patterns which are indistinguishable.

The closer muscles of the snapper and pincer claws are each innervated by two inhibitory neurones, termed the lateral and dorsal inhibitors from their cell body locations (Mellon *et al.* 1981). The lateral inhibitors of these claws, unlike the exciters, have relatively diffuse branching patterns (Fig. 5); however, like the exciters all their

ventral branching is in the cortex of the ventral neuropil. Both of the lateral inhibitors of the snapper and pincers have branches at similar locations which enter contralaterally homologous regions of neuropil. The similarity is such that even the average diameter of their primary neurites and axons is the same (neurites: snapper 10·8 μm S.D. 4·0, pincer 11·9 μm S.D. 8·04; axons: snapper 16·2 μm S.D. 3·9, pincer 16·6 μm S.D. 3·1). Similarly, when the dorsal inhibitors were compared, no consistent difference was found in the extent of branching. Fig. 5C, D illustrates the most extreme differences we saw between individuals of all four types of neurones in all the animals which we studied. The average diameters of the neurites and axons (neurites: snapper 7·8 μm, S.D. 1·9; pincer 7·5 μm, S.D. 2·2; axons: snapper 15·5 μm, S.D. 2·6; pincer 16·0 μm, S.D. 2·2) are the same. The dorsal inhibitors, like all the other claw closer neurones, have all their ventral branching in the cortex of the ventral neuropil, but unlike the lateral inhibitors they also branch within the tracts of the dorsal neuropil.

The reconstructions in Figs. 4 and 5 reveal an apparent enrichment of the higher-order dendritic branching patterns in snapper motor neurones, compared to their homologues. The disparity is most apparent with respect to homologous dorsal and lateral inhibitory neurones. Part of this difference is due to the preparations which we have chosen to present. Visual comparison of the pincer exciter 1 neurone in Fig. 4, for example, with the snapper exciter 1 neurone shown in Mellon *et al.* (1981) provides the opposite impression, namely the pincer neurone appears to have more fine branches than the snapper neurone. The apparent difference in the number of higher-order branches, furthermore, was quantified by counting all the higher-order branches in two snapper and two pincer exciter 1 motor neurones, and a 4% difference in the average number of branches was found; one snapper exciter 1 had the largest number of higher-order branches and the other had the lowest number of higher-order branches. Thus, although we cannot rule out the possibility that in the general population of snapping shrimp there may be a consistent difference in higher-order branching patterns, for the present we conclude that the features of dendritic anatomy revealed by our reconstruction techniques are similar for homologous snapper and pincer closer muscle motor neurones.

Model. The axonal input resistances and the axonal and dendritic geometries for contralaterally homologous neurones are thus very similar. However, the effect of the previously reported differences in cell body size (Mellon *et al.* 1981) upon the electrical properties of the neurones has not been examined. To determine what effect these differences in cell body size could have on the electrotonic properties of any of the neurones, we modelled the closer exciter motor neurones, using the methods of Graubard & Calvin (1979), Turner & Calvin (1981) and Calvin (personal communication). We reconstructed the voltage (PSP) decrement, for unit conductances applied at various sites on the neurone, and the axonal input resistance for model neurones with cell bodies of the sizes reported for pincer and snapper closer exciters, using the equations of Rall (1959). We found differences between such model neurones of less than 1% in PSP decrement and 3% in axonal input resistance, for R_m varied in the computations between 800 and 50,000 ohm cm^2, and cell body diameters of 60 and 75 μm (these being mean diameters for the pincer and snapper closer exciters, respectively.) Values of R_m calculated from our experimental determinations of the

length constant, λ = 1·2 and 2·2 mm, and axon radius, a = 12·5 μm (measured from tissue fixed in glutaraldehyde so as to minimize shrinkage due to treatment with ammonium sulphide and subsequent fixation in formalin), using the formula $R_m = 2\lambda^2 R_i/a$ (for a semi-infinite cable) with an assumed figure for R_i of 90 ohm cm, are 2070 and 6970 ohm cm^2. In the computer reconstruction, R_m values of 2000 and 7000 ohm cm^2 yielded input resistances of 1·3 and 3·0 MΩ, respectively, which are well within the experimentally observed range (1·2–8·0 MΩ, or 1·2–6·6 MΩ for the closer exciter neurones). Furthermore, for the two neurones whose length constants were measured, one neurone had an observed input resistance of 3·0 MΩ and a modelled value of 1·3 MΩ, while the other had an observed value of 5·0 MΩ and a modelled value of 3·0 MΩ. We thus find good agreement between the reconstruction and our data, because the model yields values for input resistances at the axon similar to those obtained experimentally, using values for R_m which were determined using independent physiological techniques and the anatomy of the neurone. We conclude that the passive electrical properties of contralaterally homologous snapper and pincer neurones are to all intents and purposes identical.

DISCUSSION

Our studies have revealed a basic similarity in the anatomical and electrical properties of the motor neurones of homologous pincer and snapper closer muscles in *Alpheus*. This is surprising, for the normal behavioural repertoires of the two claws are remarkably different.

Both Ritzmann (1974) and ourselves, however, occasionally observed the pincer claws being used in a snapping-like behaviour. These observations suggest that the motor programme for 'snapping' is available to both sets of claw closer and opener motor neurones. Since the abortive pincer 'snaps' do not accompany similar activity occurring in normally functioning snapper claws, it is apparent that the animal has complete control over which claw exhibits a particular behaviour. It is far from clear, however, by what mechanisms the behavioural bias is switched during transformation. Our failure to find anatomical or electrical differences in homologous motor neurones to the claw closer muscles suggest the possibility of changes occurring in sensory neurones or higher-order interneurones.

One possibility is the reflex circuit which is driven by dactyl abduction (claw opening) through the propus-dactyl (P–D) chordotonal organ. Ritzmann (1974) discovered that passive opening of the snapper claw was reinforced by this reflex loop, which directs positive feedback on to the claw *opener* muscle via the P–D organ. Furthermore, only in the fully opened (cocked) position of the dactyl are trains of nerve impulses generated in the closer exciter motor neurones. The snapper P–D organ is thus apparently instrumental both in opening the claw and in gating central excitation to the closer motor neurones. In the pincer claw the positive opening reflex is also present (Ritzmann, 1974), but the train of closer exciter impulses released after the dactyl opens is shorter and weaker than in the snapper. Ritzmann concluded that changes in the claw structure and its closer muscle are sufficient to account for behavioural transformation. He predicted that the 'opener reflex needs only to be

supplemented for the pincer closer exciter motor neurones to generate impulses at the same frequencies as the snapper exciter'. An important nervous modification which may accompany claw transformation is therefore the enhanced effect of P–D organ input in the control of closer motor neurones excitability. In theory this could be accomplished simply by peripheral modifications during the change in claw size and morphology. Another observation of potential importance is that, while the snapper claw is normally held fully closed, the pincer is held at 5–10° from full closure. Furthermore, this posture is maintained without tonic spiking of the excitatory motor neurones. This difference in posture may be expected to cause different tactile information to be transmitted to the ganglion from the hairs located between the dactyl and the propus, as well as causing the 'set point' of the P–D organ to be different. The change in the position of these sensory hairs caused by the morphological transformation of the claw, and the different set point or strength of response of the P–D organ, are peripheral modifications which may play a role in the behavioural changes observed in the claws at transformation.

The distribution of the major dendritic arbours of excitatory and inhibitory motor neurones is interesting. As in the crayfish (Wiens, 1974), the closer exciters of *Alpheus* form opposing, crescent-shaped, primary branches within the lateral neuropil, from which emerge many short secondary tufts. The placement of this crescentic arbour is superficial within the ventral neuropil, in that all the banches are confined to a band on the cortex of this elipsoidal structure (cf. Figs. 2–5). Within this region there is considerable overlap with the much more diffusely organized dendritic fields of the antagonists of the exciters, the two inhibitory neurones. This arrangement suggests the presence of common sources of synaptic input to these antagonist neurones, as occurs in other preparations (Burrows & Horridge, 1974; Wilson, 1979). Close-apposition of dendritic branches would seem to be especially important, for reasons of PSP decrement, when the motor neurones are targets of non-spiking interneurones (see Burrows, 1980). In these cases, overlapping fields would ensure optimally effective local processing.

We thank Ms Karen Cobb and Patricia Wilson for maintaining the animals. Dr Christine E. Phillips is thanked for fixing the tissue used in Fig. 2. Dr Robert Huskey is thanked for the use of his microscope. We would particularly like to thank Dr William H. Calvin for his invaluable help in modelling the neurones. This project was supported by U.S.P.H.S. grant number NS-15006 (to DeForest Mellon).

REFERENCES

BURROWS, M. (1980). The control of sets of motoneurones by local interneurones in the locust. *J. Physiol.* **298**, 213–233.

BURROWS, M. & HORRIDGE, G. A. (1974). The organization of inputs to motoneurones of the locust metathoracic leg. *Phil. Trans. R. Soc.* B **269**, 49–94.

GOVIND, C. K. & LANG, F. (1981). Physiological identification and asymmetry of lobster claw closer motoneurons. *J. exp. Biol.* **94**, 329–339.

GRAUBARD, K. & CALVIN, W. H. (1979). Presynaptic dendrites: implications of spikeless synaptic transmission and dendritic geometry. In *The Neurosciences, Fourth Program* (ed. F. O. Schmitt and F. G. Warden), pp. 317–331. Cambridge, Mass.: M.I.T.

KUSANO, K. (1967). Electrical activity and structural correlates of giant nerve fibers in *Kuruma* shrimp (*Penaeus japonicus*). *J. cell. Physiol.* **68**, 361–384.

McVEAN, A. R. (1974). The nervous control of autotomy in *Carcinus maenas*. *J. exp. Biol.* **60**, 423–436.
MELLON, DEF., JR. (1981). Nerves and the transformation of claw type in snapping shrimps. *Trends in Neurosci.* **4**, 245–248.
MELLON, DEF., JR. & KAARS, C. (1974). Role of regional cellular geometry in conduction of excitation along a sensory neuron. *J. Neurophysiol.* **37**, 1228–1238.
MELLON, DEF., JR. & STEPHENS, P. J. (1978). Limb morphology and function are transformed by contralateral nerve section in snapping shrimp. *Nature* **272**, 246–248.
MELLON, DEF., JR. & STEPHENS, P. J. (1979). The motor organization of claw closer muscles in snapping shrimp. *J. comp. Physiol.*, **132**, 109–115.
MELLON, DEF., JR., WILSON, J. A. & PHILLIPS, C. E. (1981). Shrimp motor neuron cell bodies change size and position during claw transformation. *Brain Res.* **223**, 134–140.
PRZIBRAM, H. (1901). Experimentelle Studien über Regeneration. *Arch. Entw. Mech. Org.* **11**, 321–345
RALL, W. (1959). Branching dendritic trees and motoneuron membrane resistivity. *Exp. Neurol.* **1**, 491–527.
RALL, W. (1962). Theory of physiological properties of dendrites. *Ann. N.Y. Acad. Sci.* **96**, 1071–1092.
RALL, W. & RINZEL, J. (1973). Branch input resistance and steady state attenuation for input to one branch of a dendritic neuron model. *Biophys. J.* **13**, 648–688.
RITZMANN, R. E. (1974). Mechanisms for snapping behaviour of two alpheid shrimp. *Alpheus californiensis* and *Alpheus heterochelis*. *J. comp. Physiol.* **95**, 217–236.
SILVEY, G. E. (1981). The distal limb motor neurons in the thoracic ganglion of the spiny lobster. *J. Comp. Neurol.* **200**, 579–595.
STEPHENS, P. J. & MELLON, DEF., JR. (1979). Modification of structure and synaptic physiology in transformed shrimp muscle. *J. comp. Physiol.* **132**, 97–108.
TURNER, D. A. & CALVIN, W. H. (1981). Dendritic analysis of lobster stretch receptor neurons: electrotonic properties with single and distributed inputs. *Cellular Mol. Neurobiol.* **1**, 193–215.
TYRER, N. M. & BELL, E. M. (1974). The intensification of profiles of cobalt-injected neurones in sectional material. *Brain Res.* **73**, 151–155.
WIENS, T. J. (1976). Electrical and structural properties of crayfish claw motoneurons in an isolated claw-ganglion preparation. *J. comp. Physiol.* **112**, 213–233.
WILSON, E. B. (1903). Notes on the reversal of asymmetry in the regeneration of the chelae in *Alpheus heterochelis*. *Biol. Bull. mar. biol. Lab., Woods Hole* **4**, 197–210.
WILSON, J. A. (1979). The structure and function of serially homologous leg motor neurons in the locust II. *Physiology*. *J. Neurobiol.* **10**, 153–167.